New burst criteria for loss of coolant accidents radiological consequences assessment

Tatiana Taurines, Tony Glantz, Sebastien Belon, Katalin Kulacsy, Márton Király, Richárd Nagy, Péter Szabó, Brahim Dif, Asko Arkoma

Annals of Nuclear Energy 206 (2024) 110646

Contents lists available at ScienceDirect

Annals of Nuclear Energy

journal homepage: www.elsevier.com/locate/anucene

New burst criteria for loss of coolant accidents radiological consequences assessment

Tatiana Taurines [a,*], Tony Glantz [a], Sébastien Belon [a], Katalin Kulacsy [b], Márton Király [b], Richárd Nagy [b], Péter Szabó [b], Brahim Dif [c], Asko Arkoma [c]

[a] Institut de Radioprotection et de Sûreté Nucléaire (IRSN), PSN-RES/SEMIA/LEMC, F-13115, Saint-Paul-lez-Durance, France
[b] Centre for Energy Research, Hungary
[c] VTT Technical Research Centre of Finland Ltd, Finland

ARTICLE INFO

Keywords:
Loss-of-coolant accident (LOCA)
Cladding
Burst criteria

ABSTRACT

During a loss of coolant accident (LOCA), elevated temperatures and depressurization of the primary circuit can lead to cladding ballooning and burst. In the frame of the R2CA project (Reduction of Radiological Consequences of design basis and design extension Accidents), funded in HORIZON 2020 and coordinated by IRSN (France), new burst models were developed to better evaluate the number of failed rods during a LOCA. A large literature review was performed to build various best estimate burst criteria as well as lower and upper envelopes and a conservative strain limit reduction approach. The impact of the cladding state was partially considered (only the hydrogen impact was quantified) due to a lack of data.

Experimental data were reassessed with advanced scanning methods, providing a deeper understanding of the cladding deformation occurring during ballooning and burst.

A series of validation tests were carried out with the DRACCAR and FRAPTRAN codes to compare the burst parameters (in this case temperature and strain) calculated with the new and the original burst criteria. The temperature calculated using the new burst limits was better reproduced with DRACCAR, but was more conservative with FRAPTRAN, than the values obtained using the original burst criteria of the codes. Burst strain was typically underestimated in both codes when using the new burst limits. The new criteria are therefore well suited to give a best-estimate or somewhat conservative estimate of the number of failed rods with respect to assessing the radiological consequences of a LOCA.

The need to disentangle the impact of parameters like the heating mode or the type of test (single or bundle) was outlined. More work with advanced methods is needed to evaluate test type impacts and uncertainties.

1. Introduction

Elevated temperatures and depressurization of the primary circuit can lead to cladding ballooning and burst during a LOCA. To assess radiological consequences during a LOCA, the number of failed fuel rods evaluation is a key parameter. Some of burst criteria used in the past were dedicated to predicting a best-estimate or an upper envelope of cladding strain to deal with flow blockage and assess core reflooding. This is the case of burst criteria on cladding strain (like the NUREG-630 or the EDGAR strain envelopes (Powers and Meyer, 1980; LOCA, 2009; Forgeron et al., 2000) or on true burst stress (Forgeron et al., 2000; Rosinger, 1984). This type of criteria generally leads to acceptable burst strain predictions because strain is directly included in the parameter triggering burst. Other types of burst criteria on temperature or engineering burst stress that are not directly linked to strain may allow a better prediction of burst temperature since this parameter is directly fitted. With such models strain may not be well predicted due to creep modelling high sensitivity close to burst (very high strain rates can be reached close to burst). This work is aimed to define new burst criteria based on an updated experimental database covering several test conditions with an extensive literature review to better evaluate the number of failed fuel rods during a LOCA by proposing best-estimate criteria and upper and lower envelopes to estimate the range of burst fuel rods proportion. The work was initiated in 2020 in the frame of the R2CA project (Reduction of Radiological Consequences of design basis and design extension Accidents), funded in HORIZON 2020 with the goal to

* Corresponding author.
E-mail address: tatiana.taurines@irsn.fr (T. Taurines).

https://doi.org/10.1016/j.anucene.2024.110646
Received 23 November 2023; Received in revised form 18 March 2024; Accepted 17 May 2024
Available online 27 May 2024

Table 1
General overview (cladding alloy, test type and number of tests) of the database.

AlloyTest type	Zry-4	M5/E110/Zr-1 %Nb	Zirlo/Opt Zirlo	Zry-2
Creep	78	12	0	0
T ramp	1093	55	79	12
P ramp	31	49	0	0
Total	1202	116	79	12

Table 2
Main Burst Database characteristics described with independent lines (For each testing characteristic, the number of tests/fraction of the overall database are provided – In green more than 50% of the test database, in orange more than 25%, in blue other tests).

Heating Mode	Joule Effect (direct heating)	Internal Electrical Heater	External Electrical Heater	External Infrared Heater	Nuclear
	585/41.5 %	509/36.1 %	104/7.4 %	126/8.9 %	85/6.1 %
Alloy	Zry-4	M5/E110/Zr-1%Nb	Zirlo/Opt Zirlo	Zry-2	
	1202/85.3 %	116/8.2 %	79/5.6 %	12/0.9%	
Test Type	T ramp	Creep	P ramp		
	1239/87.9 %	90/6.4 %	80/5.7 %		
Cladding state	As-Received	Pre-hydrided or/and pre-oxidized	Irradiated		
	1197/85 %	161/11.4 %	51/3.6 %		
Rod configuration	Single	Bundle			
	1013/71.9 %	396/28.1 %			
Environment	Steam	Inert			
	1160/82.3 %	249/17.3 %			

update a LOCA burst database and to define simple burst envelopes dedicated to burst occurrence predictions. Therefore, a large review of literature and IRSN unpublished burst tests was performed completed with reassessments of existing tests using advanced scanning methods. Simple models based on engineering stress and burst temperature were fitted and compared to historical and recently published models (Powers and Meyer, 1980; Meyer and Wiesenack, 2022). Finally various models were tested with two fuel performance codes (FRAPTRAN and DRACCAR), models accuracy on burst temperature and burst strain was studied.

2. Burst database reassessment

2.1. Selected datasets

Work previously published on a Zry-4 burst database from literature and IRSN data (Jacq and Taurines, 2021) was completed to about 1440 LOCA burst tests performed on most common light-water cooled reactors cladding alloys Zry-4, M5/E110/Zr-1 %Nb, Zirlo and Optimised Zirlo and Zry-2 (Table 1). More than twenty experimental programs were analysed (Massih and Jernkvist, 2015; Nagase and Fuketa, 2006; Nagy, 2018; Sawarn, 2017; Yadav, 2018; Chapman et al., 1984; Chapman, 1979; Chung and Kassner, 1978; Darchis et al., 1984; Karb et al., 1983; Markiewicz and Erbacher, 1988; Mohr, et al., 1983; Repetto, 2016; Report on Fuel Fragmentation, 2016; Stuckert et al., 2013; Stuckert et al., 2014; Stuckert et al., 2015; Stuckert, et al., 2018; Stuckert, et al., 2018; Stuckert, et al., 2018; Thieurmel, 2018; Wiehr and Harten, 1986; Wilson et al., 1993; Wilson, et al., 1983). Almost 80 % of tests were performed on Zry-4 samples under temperature ramps (rate controlled or semi-integral tests) (cf. Table 1). The main characteristics of the collected tests are compiled in Table 2.

Histograms on main burst parameters are given in Fig. 1 and percentiles are given in Table 3. Engineering burst stress (σ_e) and circumferential strain (ε_e) were calculated as follows:

$$\sigma_e = \frac{P_i(r_e - t_0) - P_e r_e}{t_0} \quad (1)$$

With

$$\varepsilon_e = \frac{C_e - C_e^0}{C_e^0} \quad (2)$$

Where P_i is the internal pressure at burst time, P_e is the external pressure at burst time, r_e the cladding external radius, t_0 the cladding thickness for as-received geometry[1] and ε_e the circumferential strain at mid-burst height (generally maximum circumferential strain). C_e is the maximum cladding external circumference at burst and C_e^0 is the initial cladding external circumference. In some references (LOCA, 2009; Jacq and Taurines, 2021) the engineering stress is approximated by $\sigma_{eapprox} = \frac{(P_i - P_e)(r_e - t_0/2)}{t_0}$. This approximation leads to an overestimation of engineering burst stresses by $(P_i - P_e)/2$ compared to Eq. (1). In the following, when data or criteria from this work are compared to literature references using this approximation, engineering stresses are corrected (using the current burst database, the fit leads to $\sigma_{eapprox} =$

[1] For irradiated or pre-oxidized claddings, the influence of the zirconia layer on burst stress and strain is not well described in literature. In this study, as-received geometry was used for engineering burst stress evaluations, the corrosion layer impact was not taken into.

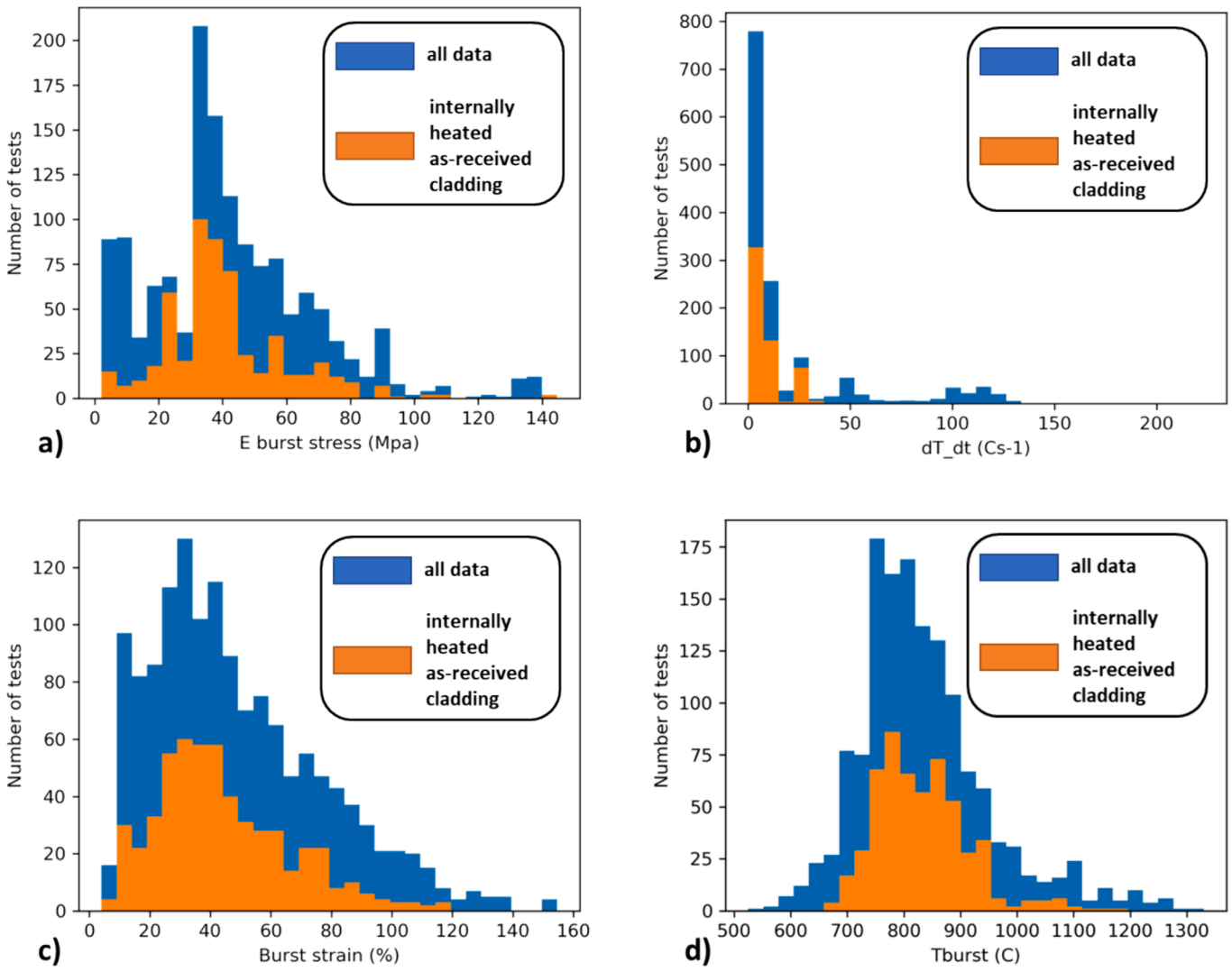

Fig. 1. Histograms of selected parameters. a) Engineering burst stress (MPa), b) Heating rate (°C/s), c) Circumferential burst strain (%), d) Burst temperature (°C). Blue all database, orange tests on as-received cladding internally heated. (For interpretation of the references to colour in this figure legend, the reader is referred to the web version of this article.)

Table 3
Some statistics about main burst parameters.

PercentileParameter	0(min)	0.1	0.25	0.5 (median)	0.75	0.9	1(max)
Tburst (°C)	525	710	757	813	889	993	1330
Heating rate (°C/s)	0	0	1	6	19	71,4	223
Engineering Burst Stress (MPa)	2.1	8.9	26.9	38.2	56.3	75.4	144.7
Engineering Circumferential Burst Strain (%)	4	16	28	43	66	89	155

$1.056 \bullet \sigma_e$ $R^2 = 0.999$).

2.2. Comparison with existing criteria

Typical burst criteria include limits on circumferential strain and stress.

- Maximum circumferential strains at burst are plotted in Fig. 2 for all heating modes or only for internal heating modes with two heating rate ranges (between 1 and 10 °C/s and above 25 °C/s). The NUREG-0630 (Powers and Meyer, 1980) envelope is also plotted for comparison in Fig. 2. These figures highlight very strong scattering in burst strain versus burst temperature, indeed similar thermomechanical loading can lead to very different ballooning behaviour and burst strains. It is known from literature that small azimuthal gradients can strongly influence bust strain (Rosinger, 1984; Karb et al., 1983), cladding state like external and/or internal oxide layer (Dominguez et al., 2022) or hydrogen content (Forgeron et al., 2000; Meyer and Wiesenack, 2022; Suman, 2021) strongly impact burst strain and/or burst temperature. The authors could not perform detailed analysis of these parameters influence since available data is not informative enough and other parameters like the experimental conditions and measurement uncertainties have a too strong impact and are entangled. The strain limits proposed in (Powers and Meyer, 1980) can be considered as an upper envelope

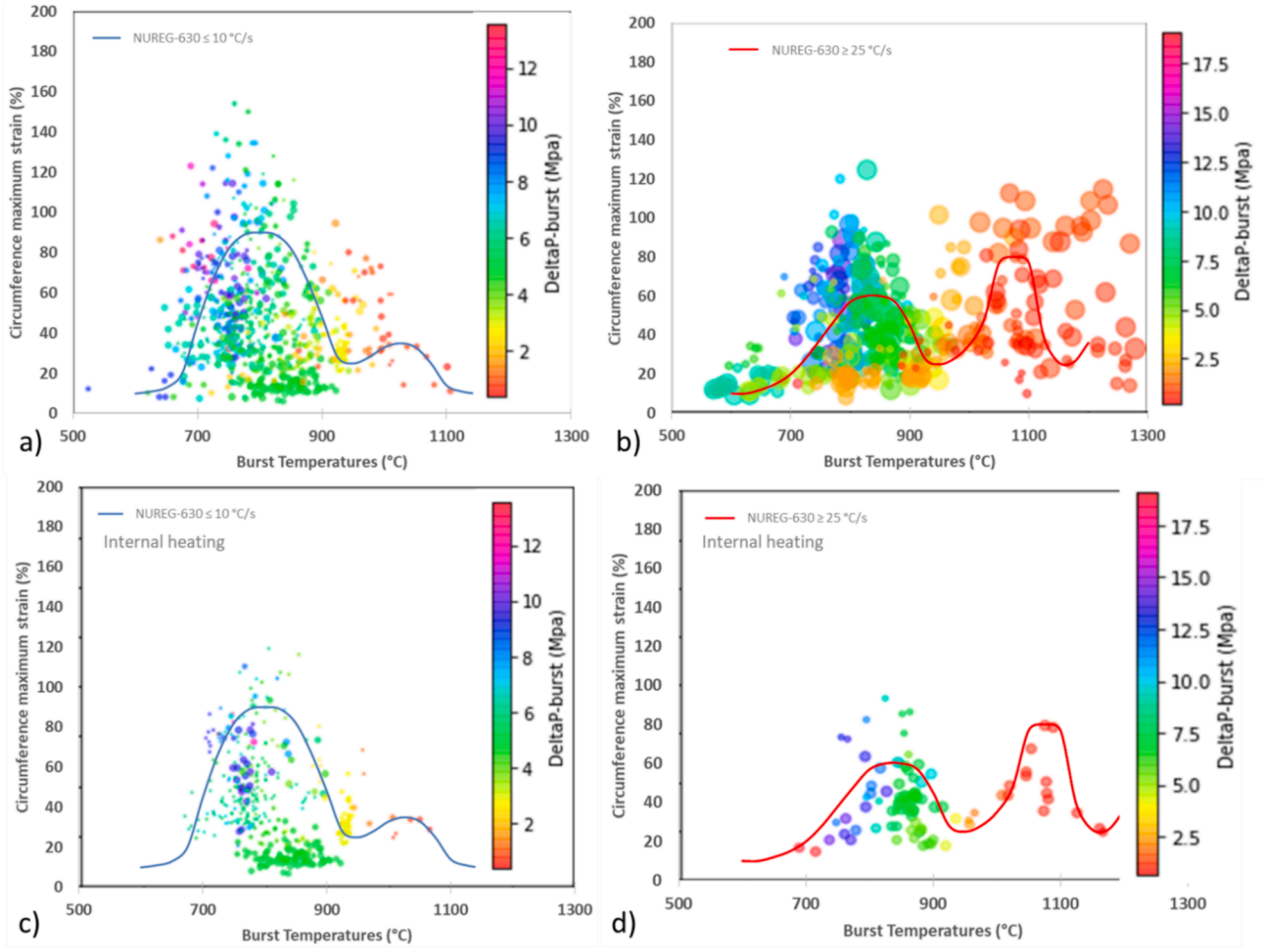

Fig. 2. Maximum circumferential burst strain versus burst temperature compared to NUREG-0630 (Rosinger, 1984) strain envelopes. a) All heating modes, heating rates between 1 and 10 °C/s, b) All heating modes, heating rates higher than 25 °C/s, c) Internal heating modes, heating rates between 1 and 10 °C/s and d) Internal heating modes, heating rates higher than 25 °C/s. Marker sizes are proportional to the heating rate.

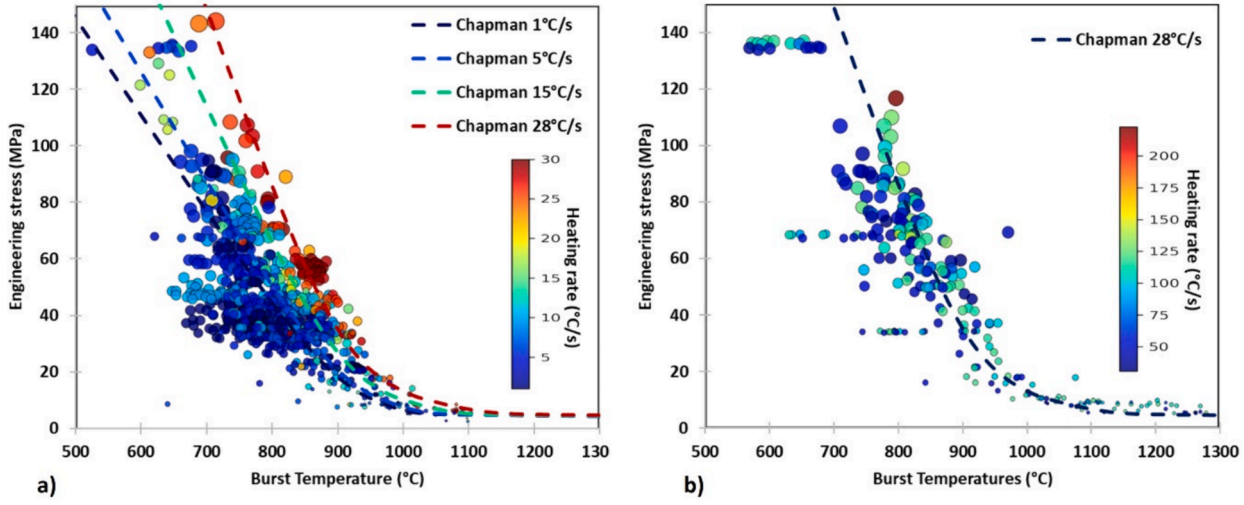

Fig. 3. Engineering burst stress versus burst temperature compared to Chapman criteria. a) Heating rates in the range 1–328 °C/s heating rate b) Heating rates in the range −28–223 °C/s.The colour map is indexed on heating rates and marker sizes are proportional to burst pressure difference.

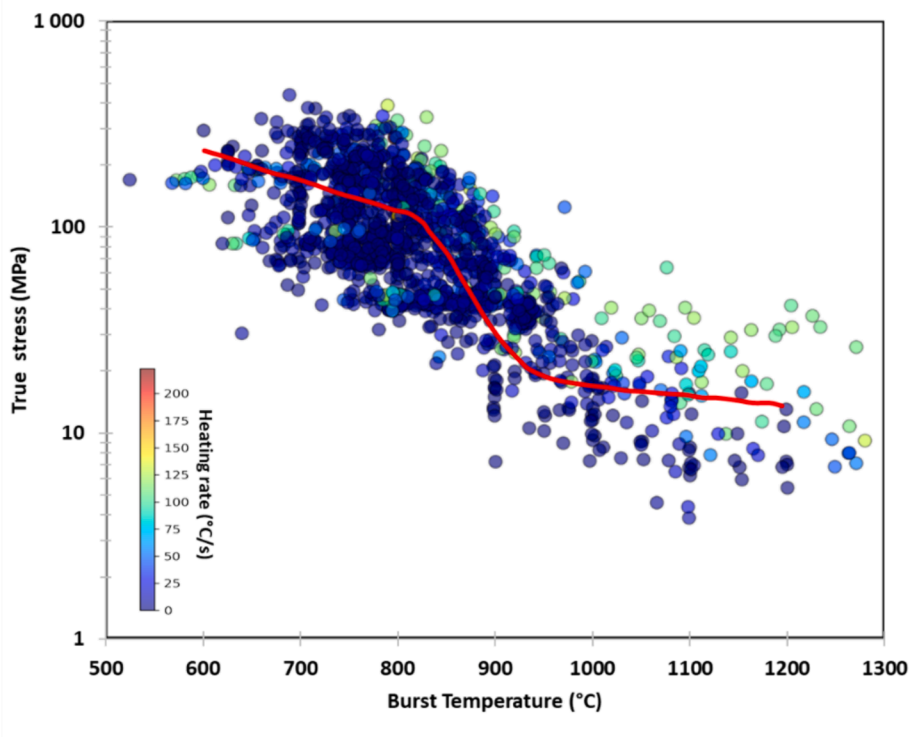

Fig. 4. True burst stress versus burst temperature with colour map on heating rate and EDGAR criterion built from creep tests (continuous line) (Yadav, 2018).

above 1000 °C for internally heated tests but not for burst at lower temperatures nor for external heating modes.

The same kind of analysis was performed on engineering stress to compare burst data with the Chapman criterion (Powers and Meyer, 1980):

$$T_{burst}\ (^{\circ}\mathrm{C}) = 3960 - \frac{20.4\sigma_{e\theta}}{1+\mathrm{H}} - \frac{8\,510\,000\,\sigma_{e\theta}}{100(1+\mathrm{H})+2790\,\sigma_{e\theta}} \quad (3)$$

Where T_{burst} is the burst temperature (°C), $\sigma_{e\theta}$ the engineering hoop stress (kpsi) and H is the ratio of the heating rate in °C/s to 28 °C/s (H varies from 0 to 1).

Figures Fig. 3a) shows that the Chapman criterion clearly overestimate burst temperature for most of the tests performed at low heating rates (<10 °C/s), tests performed around 30 °C/s are consistent with this criterion. Fig. 3b) shows that at high heating rates the shift on burst temperature saturates and that similar heating rates and pressure differences at burst can lead to a burst temperature range larger than 100 °C.

True burst stress was also analysed to look for trends and to help build a new burst criterion. The data are compared with the EDGAR criterion proposed in (Forgeron et al., 2000) from creep tests performed on Zry-4 (cf. Fig. 4). The EDGAR criterion is fairly consistent with collected data. Data scatter is very strong with burst stress differences varying within a decade.

To qualitatively illustrate the impact of the heating rate on true burst stress, data were plotted for several heating rate ranges (cf. Fig. 5). The EDGAR criterion was fitted on creep tests in isothermal conditions and is consistent with tests performed at low heating rates (cf. Fig. 5a). For higher heating rates, the data clearly shifts towards higher burst temperatures compared to the criterion. This shift could be linked to the shift of the phase transition with heating rates as reported in (Forgeron et al., 2000). Data at intermediate heating rates (cf. Fig. 5b) and d)) seems to show a simple linear behaviour, this could be due to a lack of data at high temperature.

2.3. Revisiting burst tests by detailed investigation of cladding geometry

As seen above, due to the nature of high-temperature clad ballooning, even samples tested in similar conditions may suffer significantly different total strains at burst, which gives rise to a large scatter in the experimental data. This scatter makes it extremely difficult to define the burst strain limit, which in turn increases the uncertainty of code calculations. In order to overcome this difficulty, in the framework of the R2CA project the geometry of ballooned and burst samples was studied at EK to investigate whether the local ballooning can be isolated and the burst parameters can be set up based on the remaining, uniformly expanded part of the cladding, or some other convenient method can be found to reduce the scatter. The samples were made from the Russian cladding alloy E110 containing 1 % of niobium, and the tests were performed at constant temperature and with increasing inner pressure, as recommended in references (Yegorova et al., 1999; Yegorova et al., 2001).

Two types of geometry data were used in the project that in the following will be called engineering-level data and local data. At the engineering level the geometry in a certain axial position is typically given by the total strain, from which the average thickness can be calculated, whereas the local data contain local thicknesses. All strains mentioned in this section are engineering strains, not true strains.

The total strain is usually provided in the experimental datasets, but it is not always clear what it really refers to and how it was determined. Some experimentalists (Yegorova et al., 1999; Yegorova et al., 2001) define burst strain as the strain at the tip of the crack, whereas most others (Erbacher, 1997; Perez-Feró et al., 2013) as the strain at mid-burst. The aim of the work presented here was to compare a) local thicknesses to the average thicknesses at a given axial position, and b) strains measured at several special axial positions to each other. The special positions were outside of the balloon, at the edge of the balloon, at the burst crack tip and at the middle of the burst crack.

2.3.1. Measurements made on the samples and data processing

Since the behaviour of the cladding depends on the temperature,

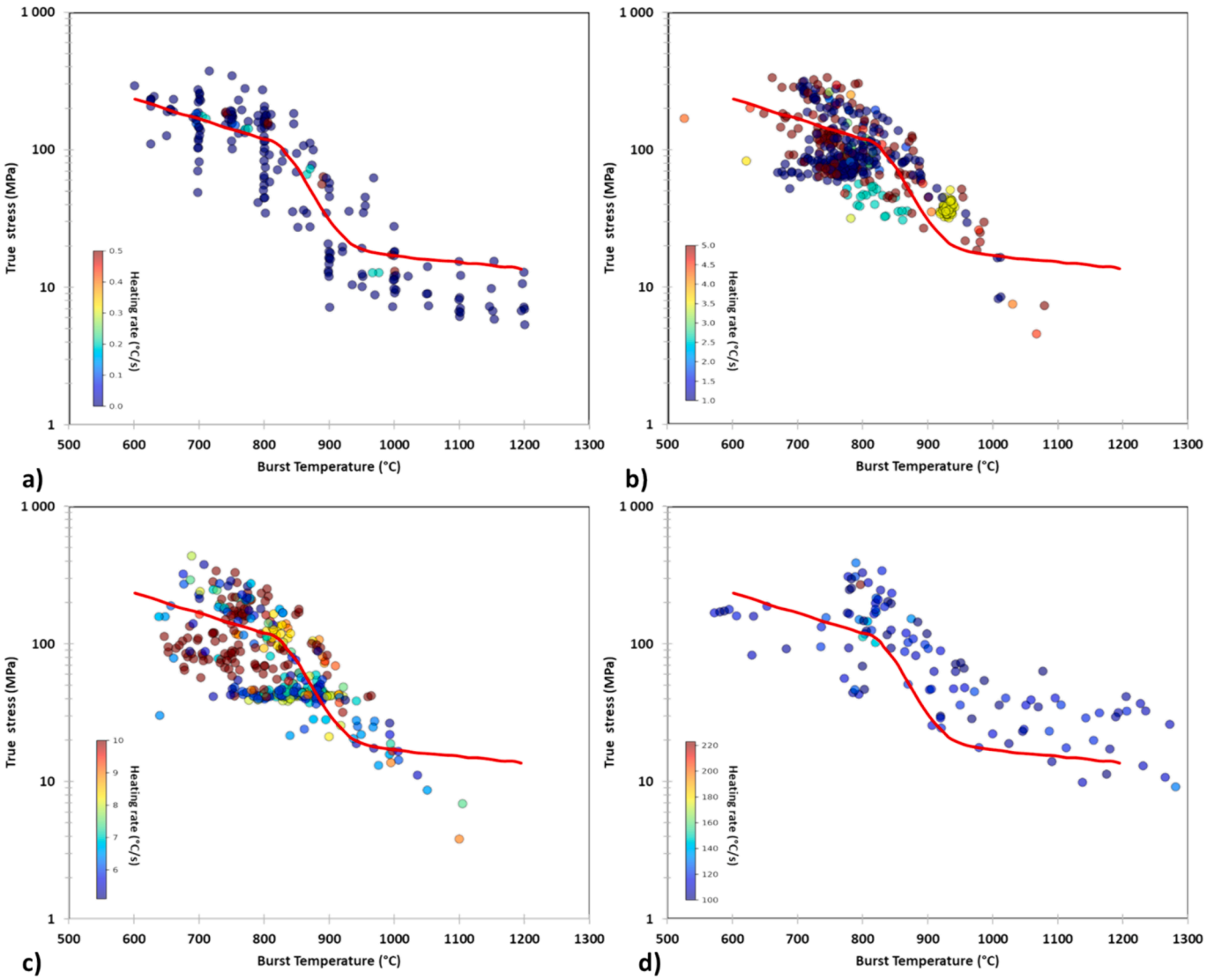

Fig. 5. True burst stress versus burst temperature with colour map on heating rate and EDGAR criterion built from creep tests (continuous line) (Yadav, 2018) a) For heating rates in the range 0–0.5 °C/s, b) For heating rates in the range 1–5 °C/s, c) For heating rates in the range 5–10 °C/s and d) For heating rates in the range 100–223 °C/s.

Table 4
Matrix of samples for the assessment of the cladding thickness at mid-burst.

	dp/dt ≈ 0.6 bar/s	dp/dt ≈ 2.7–6.6 bar/s
T ≈ 800 °C	E110	3xE110
T ≈ 900 °C	E110	2xE110
T ≈ 1000 °C	E110	2xE110
T ≈ 1100 °C	E110	–
T ≈ 1200 °C	–	E110

Table 5
Matrix of samples for the 3D CT assessment.

	dp/dt ≈ 0.5 bar/s	dp/dt ≈ 1.5–2.6 bar/s
T ≈ 700 °C	E110G slim	E110G
T ≈ 800 °C	3xE110G, E110G slim, E110	E110G, E110
T ≈ 900 °C	E110G, E110G slim	2xE110G
T ≈ 1000 °C	E110G	E110G
T ≈ 1200 °C	E110G	E110G

pressure increase rate, material, thickness, etc., two different variants of the Russian alloy (denoted as E110 and E110G or E110opt) tested at the largest possible temperature range and at very different and LOCA-relevant pressure increase rates were investigated – taking into account the availability of samples. The ballooning-and-burst tests had been performed at EK at constant temperature and constant pressure increase rate. The original inner radius of the cladding was 3.88 mm, the outer radius was 4.55 mm, except for the samples denoted by 'slim' where the outer radius was 4.45 mm. Two series of measurements were made.

In the first series twelve samples from the second part of the experimental series BALL from the AEKI database (Perez-Feró et al., 2013) were examined (cf. Table 4). The selection was based on the availability of samples, the completeness of the temperature range and the different behaviour of the cladding at very slow (about 0.5 bar/s) and relatively fast (about 2 to 6 bar/s) pressure increase rates. All of them had been cast in resin and cut at mid-burst earlier. Now a high-resolution picture was taken from each sample and points were recorded along the inner and the outer circumference, opposite each other. The coordinates were determined and the thickness was calculated in each point. The parameters of the samples are summarised in the following table.

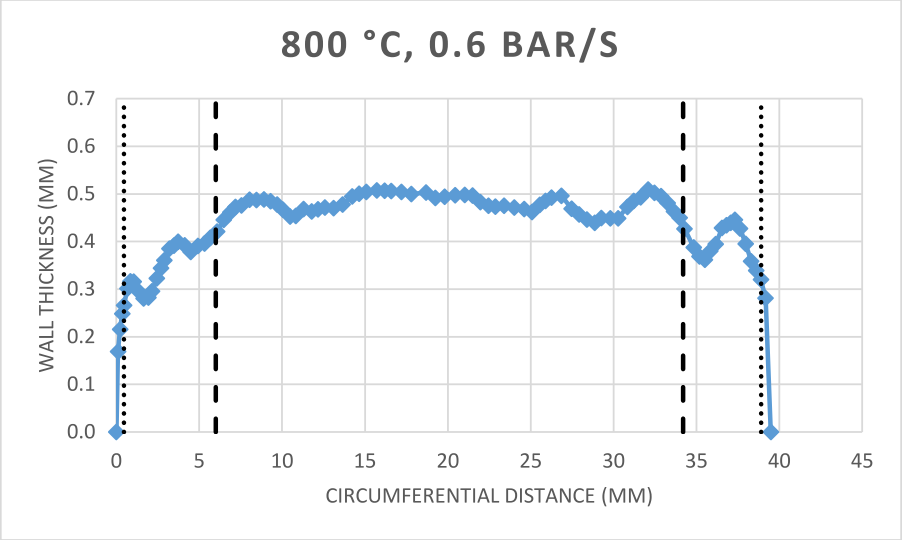

Fig. 6. Delimiting lines between burst lips, local balloon and remaining ('thick') part.

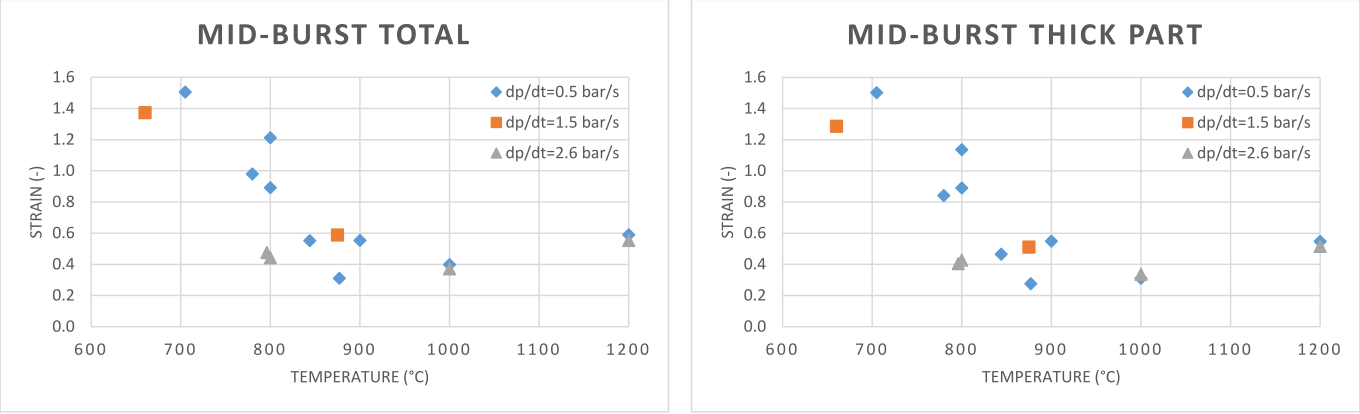

Fig. 7. Left: total strains at mid-burst, right: strains omitting the balloon.

In the second series eighteen samples from previous ballooning-and-burst experiments were subjected to a computer tomography (CT) scan, selected based on the same principles as the previous ones (cf. Table 5). The resulting gigabytes of points representing each sample were then processed in order to first determine the inner and outer surface of the cladding every 0.1 mm axially and azimuthally, and then to smooth out the noise of the measurement. In the next step straight lines were fitted at each point to the inner and the outer cladding surface and the distance between these was determined as the thickness of the cladding. Finally, the axial positions of interest (non-ballooned section, edge of the balloon, edge of the burst, middle of the burst) were determined manually and the cladding thickness data pertaining to these positions were isolated.

2.3.2. Comparison of local vs. average thickness

Classically the total circumferential elongation at mid-burst (or at the burst edge) is measured and the total strain is calculated from this. Considering how variable the shapes of the bursts and the burst lips are, there was a hope that excluding the local balloon or only the burst lips from the measurements would reduce the scatter in the burst strain data. This exclusion would mean e.g. in Fig. 6 that only the part between the dotted lines would be kept if only the burst lips were to be omitted, or the part between the dashed lines would be kept if the whole part that could be tentatively identified as the local balloon were omitted.

Fig. 7 shows the strains obtained taking into account the whole cross-section (left) and only the part without the local balloon (right). The results are not dramatically different, and, contrary to expectations, the scatter is not significantly smaller. Considering the amount of extra work necessary to obtain the local data for the reduced azimuthal length and how arbitrary it often is to determine what could be considered as the local balloon, it is not worth processing and reassessing masses of samples with this method.

2.3.3. Choice of the position where the burst strain is defined

Moving from the unballooned part of a sample towards the middle of the burst, the strain increases. The samples subjected to CT were analysed from this point of view as well. For further usability only the total strains were compared in all axial positions, so that the results can be used without massive CT scans and data processing. Fig. 8 shows the results. Some conclusions will be drawn in Section 3.3.

2.3.4. Additional outcomes of the measurements

Several features are of importance regarding Fig. 6, which also appear in the other samples:

- The thickness is very much non-uniform, even far from the burst.

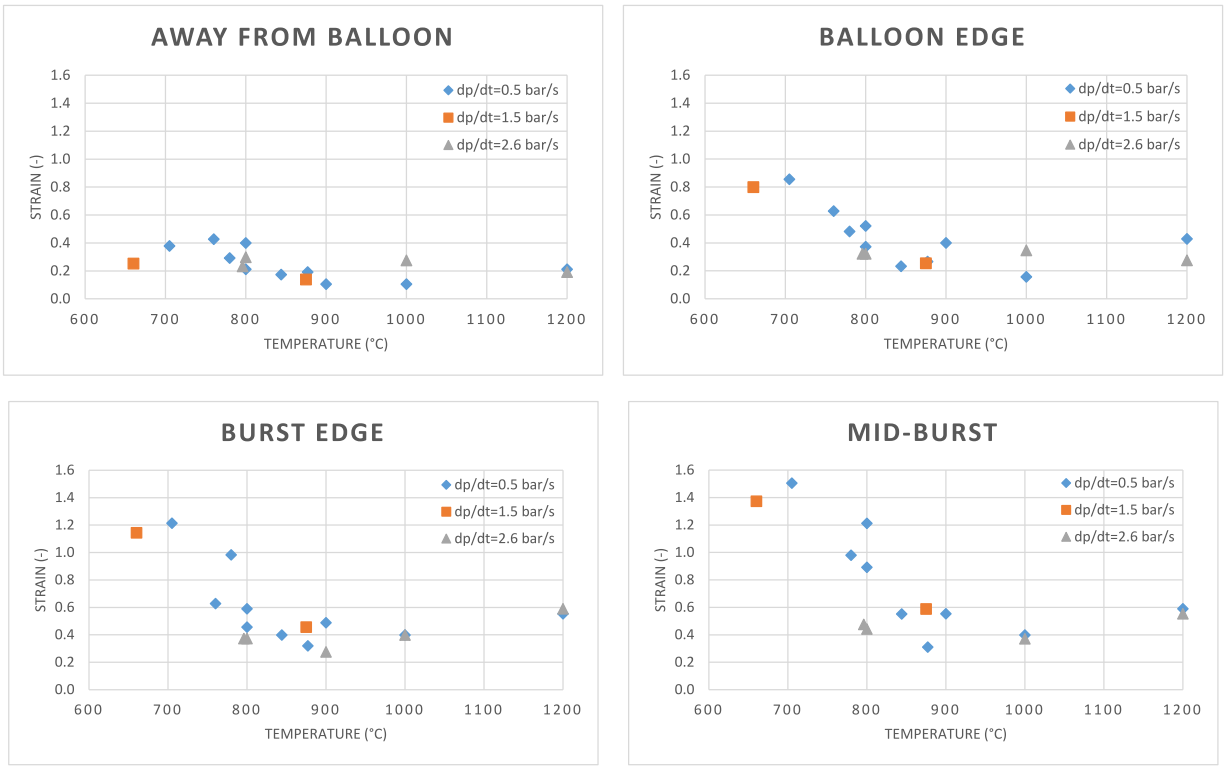

Fig. 8. Average strains in different axial positions.

Table 6
Parameters of the exponential correlations on engineering burst stress for various statistical parameters.

	σ_{min}	$\sigma_{mean-std}$	σ_{mean}	$\sigma_{mean+std}$	σ_{max}
K (MPa)	15365.53	13232.64	5928.69	5246.28	7488.42
q ($°C^{-1}$)	0.008649	0.007650	0.006085	0.005552	0.005474

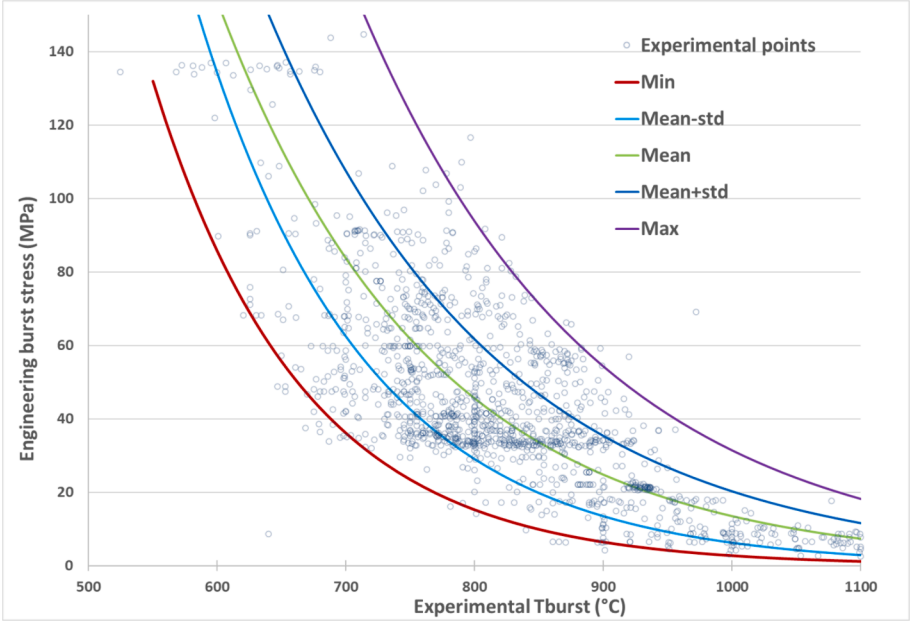

Fig. 9. Engineering burst stress versus experimental burst temperature and exponential models for statistical parameters.

Table 7
Burst temperature criterion fitting parameters for internally heated ramp tests on as-received cladding.

A (°C)	B (MPa^{-1})	C (°C/s)	D (MPa^{-1})
1145.2	27.3	16.5	0.049

- The circumference cannot be clearly divided into a thinner balloon region and a thicker, 'uniform' region that would be the non-ballooned part of the cross-section.
- There are local minima in the thickness. The sample in Fig. 6 also shows what is even more pronounced in others: the burst could have occurred in several other locations as well, probably due to local weak spots in the cladding material. This explains double ballooning in some experiments.

3. New burst envelopes and temperature criterion

During this work, simple parameters were selected to propose burst models without the need of fitting or using existing cladding thermo-mechanical models like phase transition or cladding creep. Therefore, engineering burst stress, burst temperature and the heating rate have been selected. Engineering stress is less sensitive than true stress to creep and strain measurements since it is only influenced by pressure evolution and not to geometrical changes during creep. The impact of hydrogen has been investigated and compared to literature data.

3.1. Engineering stress envelopes on the whole database

As a first approach, since no evidence of an impact in the phase transition region appears in the scatter plot envelopes on engineering burst hoop stress were fitted based on an exponential trend and considering all data points from the database (all materials and test conditions). To build these envelopes, all data were filtered in the range 700–1000 °C with a 25 °C temperature step; outside of this range there were not enough data. For each group, statistical data (minimum, mean, maximum values and standard deviation) were calculated and then each one was fitted. The exponential envelopes were of the form $\sigma_{\theta burst}(T) = K^{*}e^{-qT}$, where the parameters K and q are given in Table 6 and comparison to data is illustrated in Fig. 9. The extrapolation of the models outside of the 700–1000 °C range seems acceptable even if a slight underestimation of true burst stress is observed.

3.2. R2CA temperature criterion on internally heated tests

As shown in (Yegorova et al., 2001) the effect of irradiation on the mechanical properties of the cladding are annealed around a temperature of 800 K, i.e. approx. 650 °C. It is therefore feasible to use unirradiated samples to set up burst criteria for LOCA conditions. Based on this, a temperature criterion like the Chapman criterion (Powers and Meyer, 1980) has been fitted on as-received samples internally heated (509 temperature ramp tests performed on various alloys but mainly Zry-4), with heating rates between 0.8 and 38 °C/s (cf. Table 7). The change in the function type is due to a very large scattering of data at 1 °C/s as shown in Fig. 12a).

$$T_{burst}\ (^{\circ}C) = A - \frac{B\sigma_{e,\theta}}{1 + \frac{\min\left(\frac{dT}{dt}, 38\right)}{C} + D\sigma_{e,\theta}} \quad (4)$$

Where T_{burst} is the burst temperature (°C), $\sigma_{e\theta}$ the engineering hoop stress (MPa) and $\frac{dT}{dt}$ the heating rate (°C/s). This model is only valid for heating ramps from 1 to 38 °C/s.

The comparison between calculated temperatures and experimental temperatures is illustrated in Fig. 10.

The performance analysis of the burst criterion developed during this work is summarized in Table 8. The mean error is of 26.7 °C and more

Table 8
Burst temperature criterion performances compared to Chapman (Powers and Meyer, 1980) and Meyer (Meyer and Wiesenack, 2022) criteria for internally heated burst tests.

	R2CA temperature criterion	Chapman et al.	Meyer et al.
Mean error $\lvert T_{calc} - T_{exp} \rvert$	26.7 °C	49.6 °C	46.3 °C
Proportion of overpredicted burst temperature	52 %	61 %	71 %
Proportion of absolute temperature error lower than 50 °C	88.6 %	78.9 %	70.3 %

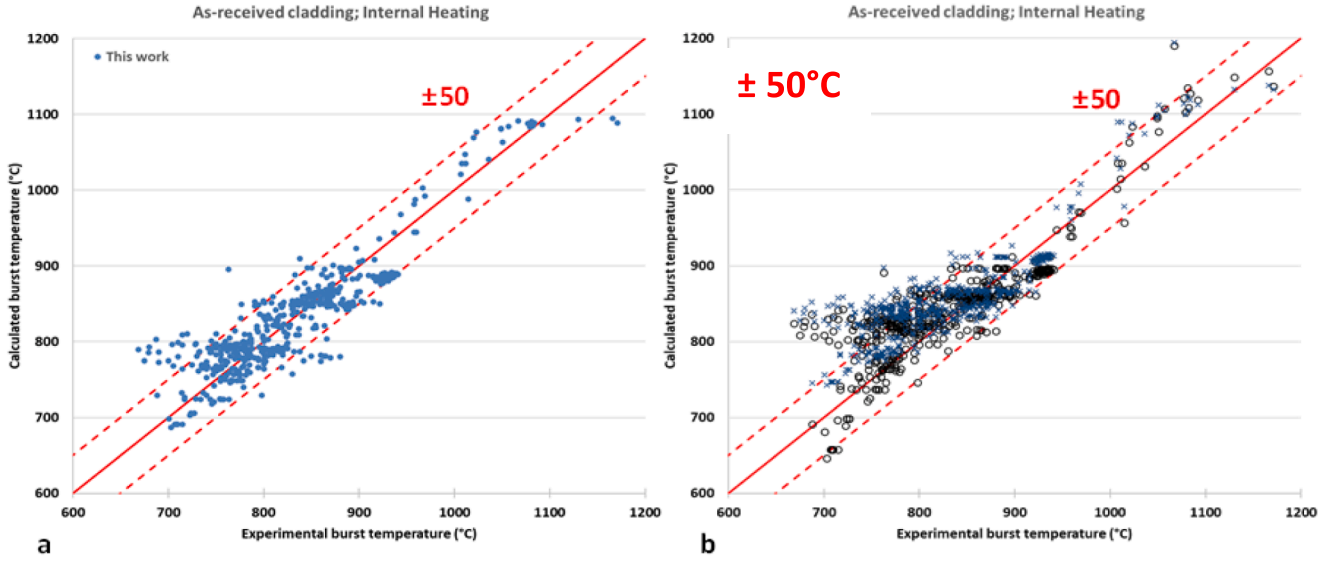

Fig. 10. Calculated versus experimental burst temperature with a) the R2CA temperature criterion, b) Chapman (Powers and Meyer, 1980) and Meyer (Meyer and Wiesenack, 2022) criteria. Dashed lines correspond to ± 50 °C from the bisector line.

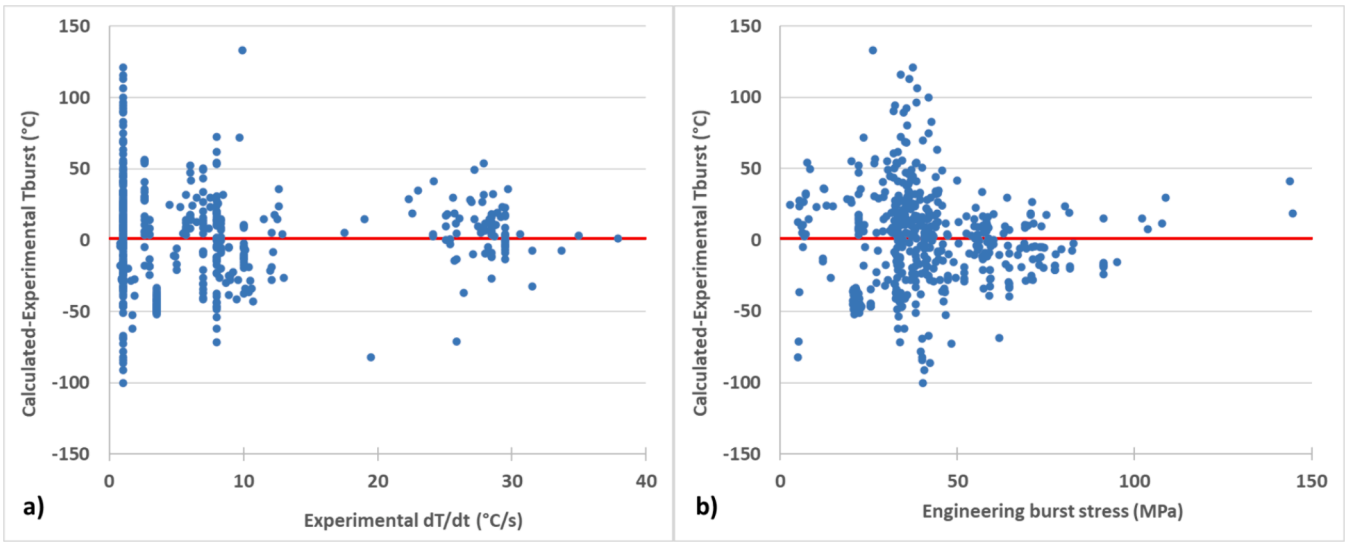

Fig. 11. Burst temperature error (calculated-experimental) versus a) the heating rate (°C/s) and b) the engineering burst stress (MPa).

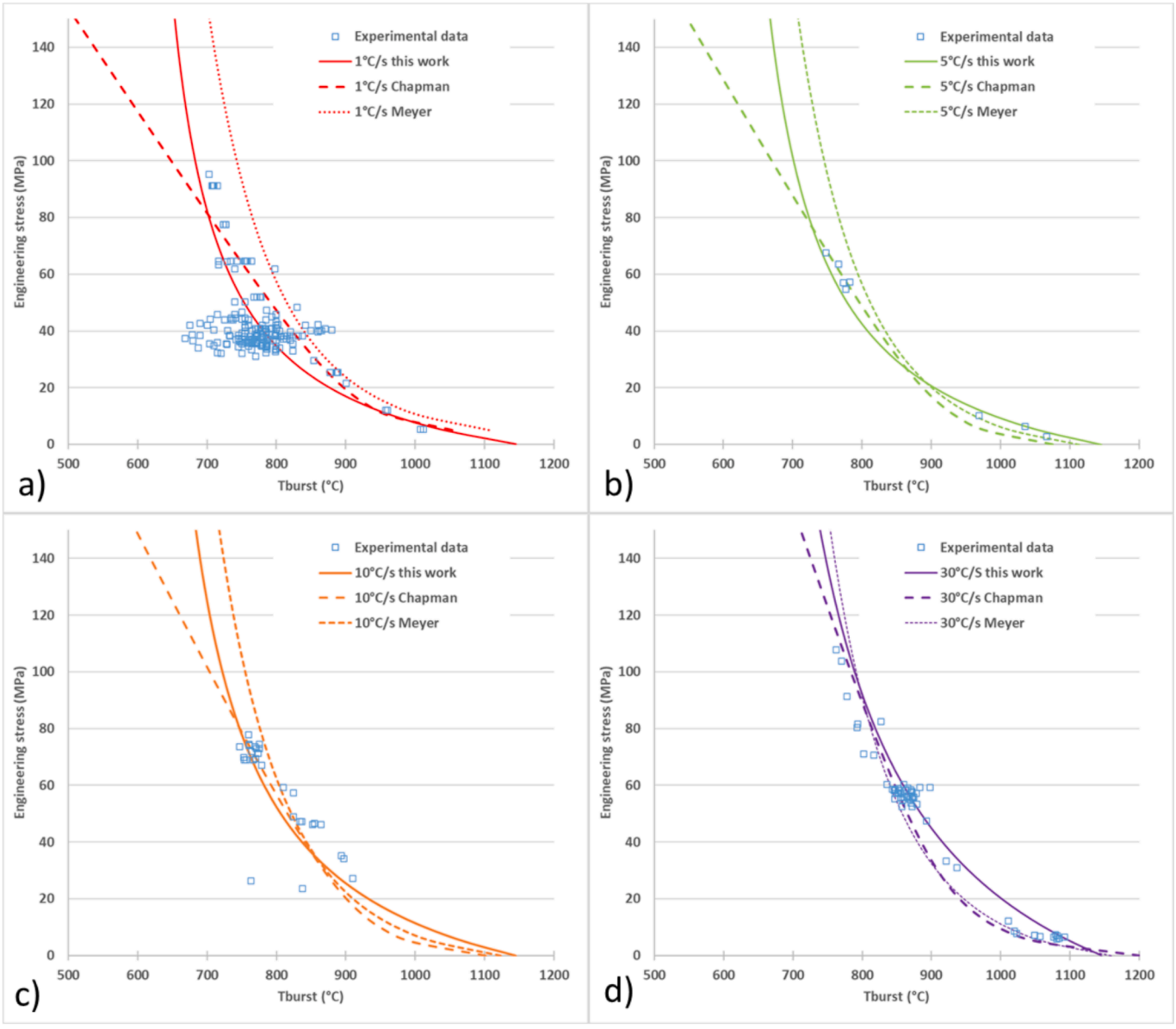

Fig. 12. Burst criterion on engineering stress developed during R2CA, Chapman criterion and Meyer criterion for heating rates of 1, 5, 10 and 30 °C/s.

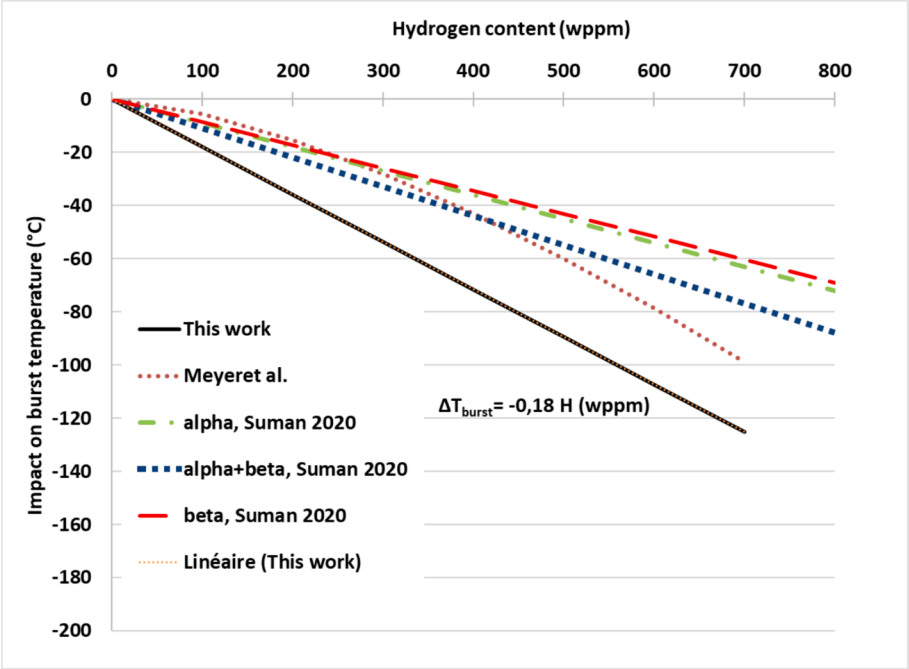

Fig. 13. Impact of hydrogen on burst temperature and comparison to literature from (Meyer and Wiesenack, 2022; Suman, 2021).

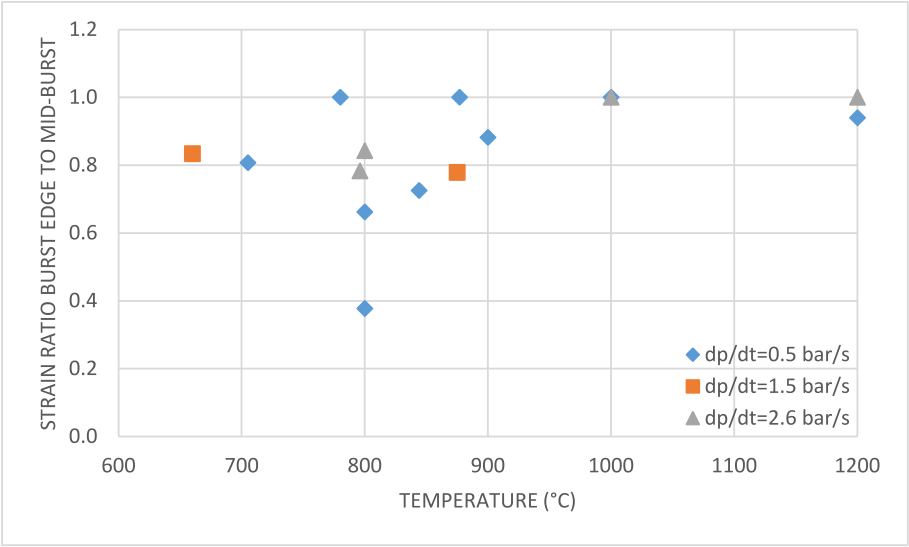

Fig. 14. Ratio of the average strain at the burst crack tip to the average strain at the middle of the burst.

that 88 % of the tests are predicted within an error lower than 50 °C. The comparison with two existing criteria shows that the new criteria is a best-estimate model with a proportion of overpredicted burst temperatures close to 50 % which is not the case for the two existing models that clearly overestimate burst temperature in particular for low burst temperatures. Nevertheless ell models fail to capture a few tests with burst temperature lower than 700 °C.

Several investigations were performed to look for groups of tests conditions poorly predicted by the model but no trends were found. For example, the error versus the heating rate or the engineering burst stress does not follow any trend as illustrated in. Fig. 11. 85 % of tests with absolute burst temperature error higher than 50 °C were performed in bundle configuration. In these tests, burst conditions could be influenced by thermal environment or measurements may be less accurate than in single configurations. The authors decided to keep bundle data in the considered database.

The R2CA temperature criterion was also compared with the Chapman criterion (Powers and Meyer, 1980) and the Meyer criterion (Meyer and Wiesenack, 2022) for various heating rates (cf. Fig. 12) and the following trends are observed:

- The stress limit versus temperature from this work and the Meyer criterion have a similar behaviour, with a sharp decrease of burst stress in the range 700–750 °C. In particular for heating rates lower than 10 °C/s.
- The difference between the three criteria decreases with increasing heating rates.
- At high engineering stresses (above ~ 80 MPa), burst temperature predicted with the R2CA criterion is between the ones predicted by Chapman and Meyer criteria.

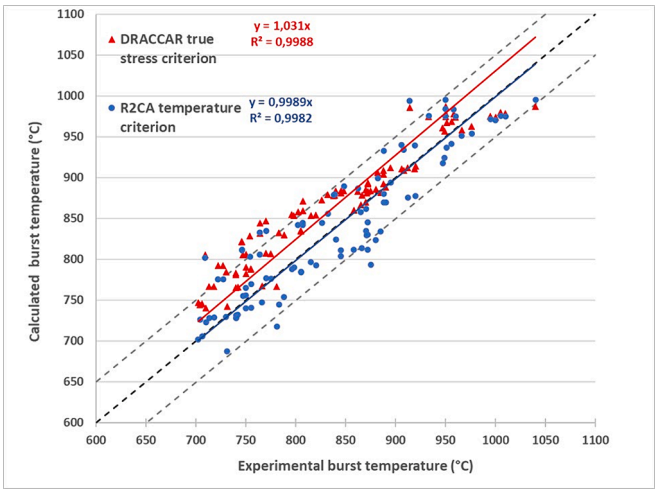

Fig. 15. Calculated burst temperature versus experimental temperature on EDGAR test on Zry-4 with DRACCAR true stress criterion and R2CA temperature criterion and linear fitting (y = ax). Gray dashed lines correspond to ± 10 %.

- At 1 °C/s, the R2CA criterion predicts lower burst temperatures than the two other criteria.
- For low stresses (<20 MPa) the R2CA criterion predicts higher burst temperatures than the two other criteria, in particular at 30 °C/s.

As mentioned in the introduction, hydrogen content leads to lower burst temperatures. 35 tests with hydrogen content up to 750 wppm were analysed to quantify the impact on burst temperature which leads to:

$$\Delta T_{burst}\ (^{\circ}C) = -0.18\,H(wppm),\ 0 < H > 750\,wppm \quad (5)$$

A comparison with published correlations from literature is illustrated in Fig. 13, the correlation proposed in this work leads to a higher impact of hydrogen on burst temperature. It may come from the fact that considered data mix various experimental programs which was not the case in references (Meyer and Wiesenack, 2022) or (Suman, 2021). More data is necessary to better quantify the impact of hydrogen content in various cladding thermomechanical loadings.

3.3. E110 strain criterion

The edge of the burst crack represents the area where local instability starts, therefore based on the information presented in Section 2.3 it has been decided to use it as an alternative to the middle of the burst. The scatter of the data is not reduced considerably by using the strain at the edge of the burst instead of the middle, only the absolute values are, as summarised in Fig. 14. If the edge of the burst is considered instead of the middle, the reduction in strain is in almost all the cases above 60 %.

The measured average strains at mid-burst or any curve fitted to these can be used as a best-estimate strain, e.g. to fit the mechanical models of the codes. A reduction to 60 % of this value (which corresponds to a conservative representation of the strain at the burst crack tip) can then be used as a conservative burst strain for the evaluation of the number of failed fuel rods in a LOCA scenario.

4. The effect of the new burst criteria on validation test cases

4.1. Validation of DRACCAR on selected tests

DRACCAR is a 3D computational tool dedicated to simulating reflooding with channel blockage during LOCA (Glantz et al., 2017; Glantz et al., 2017). It allows a direct coupling between the thermo-mechanical behaviour of the fuel assembly and the thermal hydraulics. The thermo-mechanical behaviour of fuel rods considers cladding creep, ballooning, burst and axial fuel relocation. Various burst criteria were available in the code before the R2CA project, but most of them are

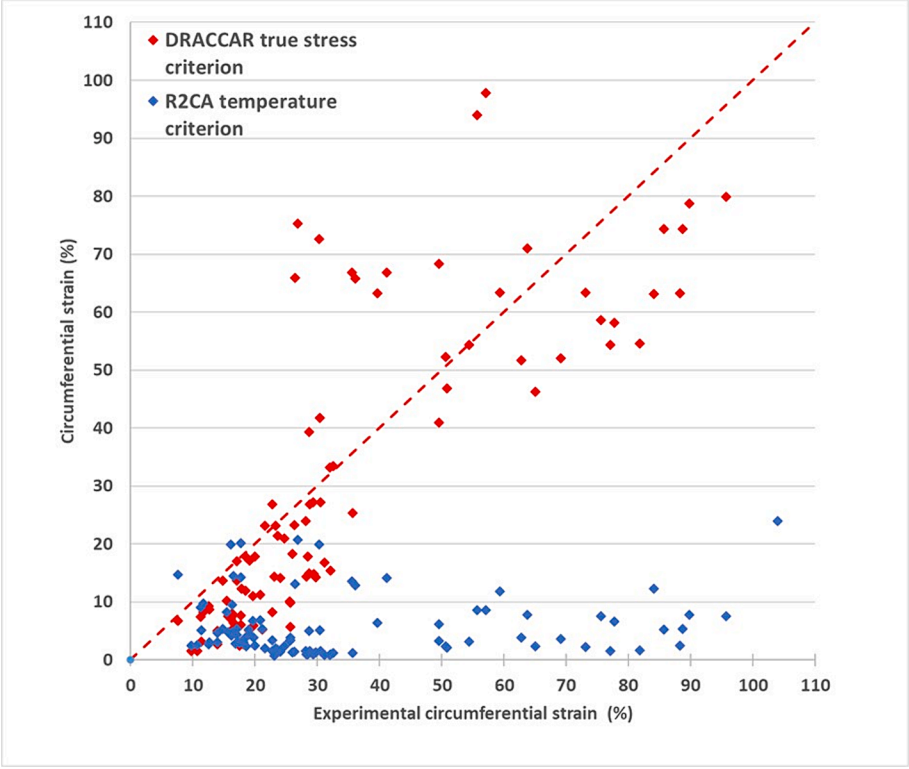

Fig. 16. Calculated circumferential strain versus experimental circumferential strain for temperature ramp tests.

Table 9
Validation cases for FRAPTRAN-VTT1.4.

LOCA test	Average heating rate (°C s^{-1})	Measured cladding T at burst (°C)	Calculated burst temperature (°C)			
			FRAPTRAN original criterion	R2CA engineering stress mean envelope	R2CA temperature criterion	Meyer & Wiesenack 2022
IFA-650.5	5.0–5.5	750	781	732	732	725
IFA-650.6	1.7–1.9	830	813	793	766	801
IFA-650.7	9	1100	948	948	948	948
IFA-650.15	5.6—5.8 °C s^{-1} until ballooning then 2.6 °C s^{-1} for the remaining heat-up phase	800	781	724	719	760
LOC-11Crod 3	80–90 °C s^{-1} until 5 s then 11–12 °C s^{-1} for the remaining heat-up	No burst	No burst	No burst	740	No burst
LOC-11Crod 2		No burst	No burst	No burst	752	No burst
LOC-11Crods 1 and 4		No burst	No burst	No burst	No burst	No burst

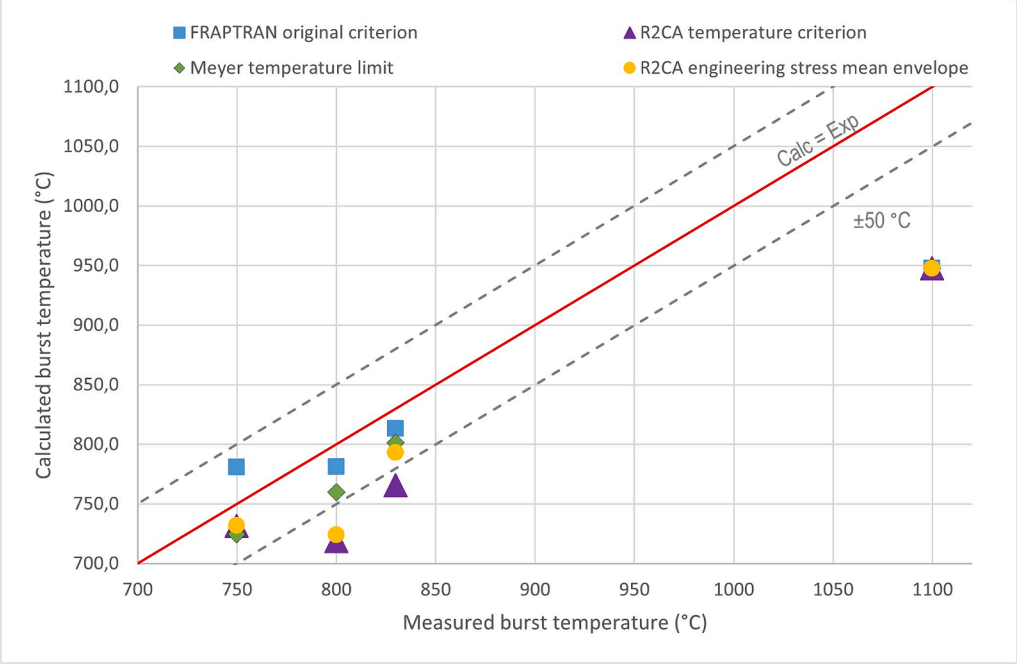

Fig. 17. Calculated versus experimental burst temperature for the simulated validation cases. Dashed lines correspond to ± 50 °C from the bisector line.

dedicated to predict/envelop cladding strain for flow blockage considerations. The available criteria in DRACCAR are strain limits, temperature limits, true stress limits.

To test the newly developed criterion on burst temperature, the DRACCAR code developed at IRSN was run on tests not used in the validation database. This study was performed on 125 LOCA-relevant transients performed on Zy-4 cladding directly heated by Joule effect with temperature heating rates between 0.1 and 100 °C/s and imposed internal pressures ranging from 10 to 130 bar (EDGAR tests (LOCA, 2009; Forgeron et al., 2000; Darchis et al., 1984).

. Calculated burst temperatures versus experimental burst temperatures are illustrated in Fig. 15. The R2CA temperature criterion leads to best estimate predictions whereas the true stress burst criterion generally overestimates burst temperature. For both cases predictions are within ± 10 % of experimental burst temperatures. The mean absolute errors are similar, 29 °C for the R2CA temperature criterion and 32 °C for the DRACCAR true stress criterion but with a quasi-systematic temperature overprediction.

To conclude on DRACCAR simulations versus experimental results, the R2CA temperature criterion based on engineering stress allows a better evaluation of burst temperatures than the criterion used in the DRACCAR validation tests based on true stress. For the studied cases, the use of the R2CA temperature criterion led to three burst occurrences experimentally not observed (over 125 tests), whereas the use of the DRACCAR true stress criterion led to miss two burst predictions. Overall, the use of the R2CA temperature limit based on engineering stress leads to better burst temperature evaluations for the cases considered in this study. However, the burst criterion based on engineering stress is not well-suited to predict burst cladding strain as illustrated in Fig. 16. Indeed, for most of the cases the calculated strain is significantly underpredicted with the R2CA criterion. This could be explained by the fact that strain is not a parameter in the criteria to trigger burst, and that strain rates are very high close to burst time. Other burst parameters were compared to the experimental values, it showed that burst time prediction is very close to the DRACCAR criterion and that short times shifts can lead to significant differences in final calculated strain.

4.2. *Validation of FRAPTRAN on selected tests*

The R2CA temperature limit criterion and the R2CA mean engineering stress limit were implemented in FRAPTRAN-VTT1.4. The modified version of the code computes mechanical deformation in the ballooning region based on a high temperature creep law. In this approach, the original plastic strain component is replaced by a creep

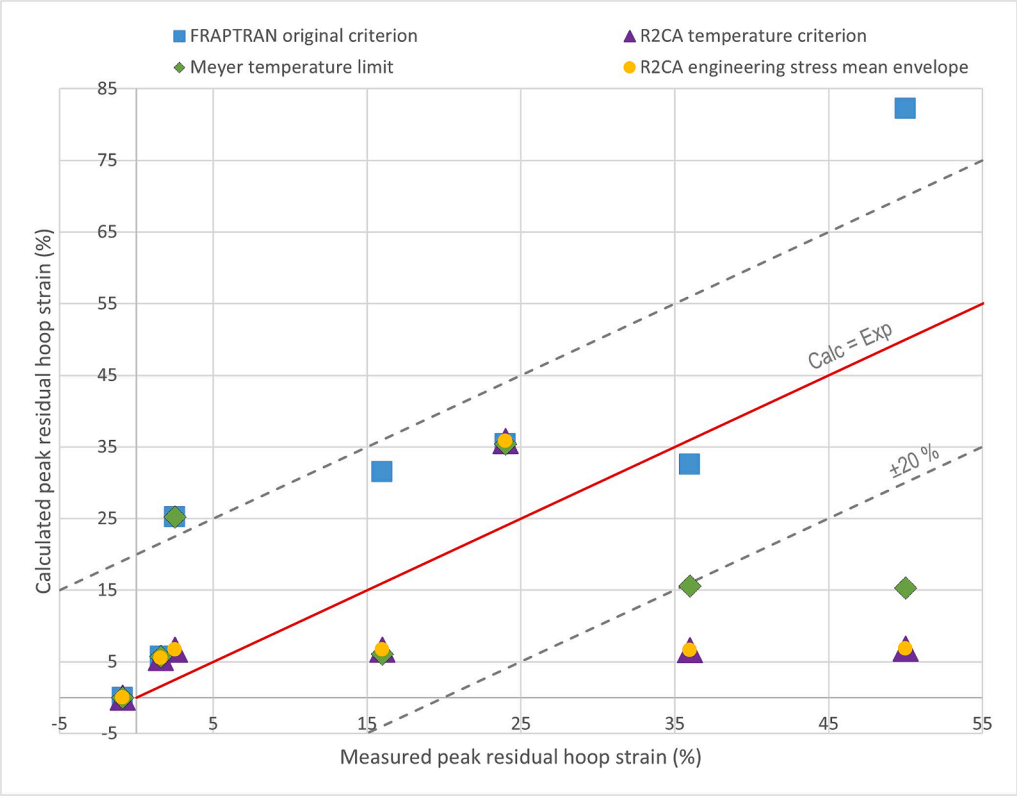

Fig. 18. Comparison of FRAPTRAN-VTT1.4 calculated versus experimental peak residual hoop strains following LOCA tests. Dashed lines correspond to ± 20 % from the bisector line.

Table 10
Comparison of FRAPTRAN-VTT1.4 predicted vs measured peak residual hoop strains following LOCA tests.

LOCA test	Average heating rate (°C s^{-1})	Measured peak residual hoop strain. (%)	FRAPTRAN-VTT1.4 peak residual hoop strain (%)			
			FRAPTRAN original criterion	R2CA engineering stress mean envelope	R2CA temperature criterion	Meyer & Wiesenack 2022
IFA-650.5	5.0–5.5	16	31.5	6.6	6.7	6.1
IFA-650.6	1.7–1.9	36	32.5	12.0	6.6	15.6
IFA-650.7	9	24	35.4	35.8	35.8	35.4
	5.6–5.8 °C s^{-1} until ballooning then 2.6 °C s^{-1} for the remaining heat-up phase	50	82.2	6.3	6.8	15.3
LOC-11Crod 3	80–90 °C s^{-1} until 5 s then 11–12 °C s^{-1}	1.6	5.7	5.7	5.5*	5.7
LOC-11Crod 2	for the remaining heat-up	2.5	25.2	25.2	6.7*	25.2
LOC-11Crods 1 and 4		−0.96 and −0.84	0.02	0.02	0.02	0.02

*Burst is predicted during the 11–12 °C s^{-1} heat ramp.

strain calculated using Norton formulation and a phase transformation model (Massih, 2009), unlike the original plasticity model used in the U. S. NRC's FRAPTRAN 1.4 version. This development, along with the implementation of different LOCA burst criteria, was carried out within the R2CA project. (Dif, 2023). Creep strain rate ($\dot{\varepsilon}_{creep}$) is given by (Kaddour, 2004):

$$\dot{\varepsilon}_{creep} = \frac{A}{T}\sigma^{n}\exp\left(-\frac{Q}{RT}\right) \quad (6)$$

Here, A is the strength coefficient, T is the temperature, Q is the activation energy, R is the gas constant and n is the stress exponent.

To test the newly implemented burst criteria, a few validation cases were selected from the FRAPTRAN LOCA integral assessment database. In addition, one more case was added from the Halden LOCA test series, the IFA-650.15 with M5 cladding. The test cases are summarised in Table 9.

Two high-temperature creep models, proposed by Kaddour et al. (Kaddour, 2004) and Rosinger (Rosinger, 1984), were implemented to FRAPTRAN-VTT1.4. For the comparison of various burst criteria, the Kaddour et al. model was selected due to its demonstrated advantage in producing better predictions of burst compared to FRAPTRAN's original plasticity model and the Rosinger model. Kaddour et al. model also provides specific creep parameters for both Zry-4 and M5 cladding types, unlike the other two deformation models. The results of calculations for burst temperature and residual strain are presented in Fig. 17 and Fig. 18, respectively. The results show burst predictions from four different criteria: FRAPTRAN original criterion, R2CA temperature criterion, R2CA engineering stress mean envelope (Table 6) and the temperature criterion by Meyer and Wiesenack (Meyer and Wiesenack, 2022).

Additionally, it is worth noting that FRAPTRAN inherently predicts burst under LOCA conditions based on true stress calculations. When

ballooning occurs, FRAPTRAN predicts burst when the local true hoop stress in the ballooning node exceeds an empirical true stress limit provided by MATPRO. However, to consistently implement the R2CA criteria based on the engineering stress, the code was modified to calculate the local engineering stress in the ballooning node as in eq. (1).

Overall, seven validation cases were simulated. In three of these tests, the fuel rods did not rupture in the experiments. Nevertheless, the R2CA temperature criterion was the most stringent limit, falsely triggering burst for two of those cases, unlike the other criteria that showed correct predictions. The limit also produced conservative predictions in terms of burst temperature (see Fig. 16) and burst time for the other tests. Based on Fig. 12, it was expected that the R2CA temperature criterion is more conservative compared to Meyer temperature criterion in most of the cases.

Calculated burst strains were also compared to measured ones (cf. Fig. 18 and Table 10). As it turned out, FRAPTRAN's original criterion typically led to an overestimation of the strains, whereas the other three limits tended to underestimate it. The variation in predictions from different criteria were expected as there are inherent differences between all the applied criteria due to their functional forms and the applied databases used to fit the criteria.

5. Conclusions

The objective of the R2CA project was to improve the safety analysis methods in the assessment of the radiological consequences of design basis and design extension accidents. One way to do this is to improve the accuracy of the cladding burst models regarding burst occurrence (ie. Burst time and temperature) so that the number of failed rods can be evaluated more accurately. This was the subject of the present paper.

Based on experimental datasets, previous burst criteria and detailed geometrical investigation of ballooned and burst cladding samples, several new burst limits were established by different organisations taking part in the project:

a) A best-estimate limit on temperature-dependent engineering burst hoop stress was set up, together with the upper and lower envelopes of the complete dataset used to determine the limit, and the limit shifted upwards and downwards by one standard deviation. These envelopes can then be used for sensitivity analysis.
b) A best-estimate limit on engineering-hoop-stress-dependent burst temperature was determined with improved accuracy in burst occurrence prediction but with strain prediction poor capabilities.
c) A conservative reduction of the engineering burst hoop strain was proposed.

A series of validation tests was run with the codes DRACCAR and FRAPTRAN to compare the burst parameters (in this case temperature and strain) calculated with the new and the original burst criteria. The temperature calculated using the new burst limits was better reproduced with DRACCAR, but was more conservative with FRAPTRAN, than the values obtained using the original burst criteria of the codes. Burst strain was typically underestimated in both codes when using the new burst limits. The new criteria are therefore well suited to give a best-estimate or somewhat conservative estimate of the number of failed rods.

The new criteria could be used to calculate the radiological consequences of accidents in a best estimate approach. Indeed, in several countries the assumption for the assessment of radiological consequences is that 100 %, i.e. all of the rods, burst during a large-break LOCA. A sufficiently conservative failure limit used together with a best-estimate cladding deformation model ensures that the number of rods burst in the analysis will be safely conservative, so that the 100 % failure can be replaced by a lower, but still conservative number. In some countries the assumption is different, for example in France 33 % of the fuel rods are considered failed for radiological consequences evaluations.

Further analysis to disentangle the impact of parameters like the heating mode, the test type (single or bundle) or the impact of the cladding state (corrosion layers, hydrogen content) is needed. Further work with advanced methods is planned help analysing non quantitative parameters impacts and the impact of experimental uncertainties. Finally, using combined parameters in the burst criteria could help improving both burst occurrence prediction (time and/or temperature) and strain predictions but much complete data is needed (time-dependant data that is seldom available).

CRediT authorship contribution statement

Tatiana Taurines: Writing – original draft, Validation, Supervision, Methodology, Data curation, Conceptualization. **Tony Glantz:** Writing – review & editing, Validation. **Sébastien Belon:** Writing – review & editing, Validation. **Katalin Kulacsy:** Writing – original draft, Validation, Methodology, Data curation. **Márton Király:** Data curation. **Richárd Nagy:** Data curation. **Péter Szabó:** Data curation. **Brahim Dif:** Writing – original draft, Visualization, Validation, Data curation. **Asko Arkoma:** Writing – original draft, Visualization, Validation, Conceptualization.

Declaration of competing interest

The authors declare the following financial interests/personal relationships which may be considered as potential competing interests: Taurines reports financial support was provided by European Commission. If there are other authors, they declare that they have no known competing financial interests or personal relationships that could have appeared to influence the work reported in this paper.

Data availability

The authors do not have permission to share data.

Acknowledgements

This project has received funding from the Euratom research and training program 2014-2018 under grant agreement No 847656. Views and opinions expressed in this paper reflect only the author's view and the European Commission is not responsible for any use that may be made of the information it contains.

References

Chapman, R.H., A.W. Longest, and C.J. L., Experiment Data Report for Multirod Burst Test (MRBT) Bundle B-6, NUREG/CR-3460, 1984.
R. H. Chapman, Oak Ridge National Laboratory, "Multirod Burst Test Program Proqress Report for April-June, 1979," USNRC Report NUREG/CR-1023, November, 1979.
Chung, H.M., Kassner, T.F., 1978. Deformation Characteristics of Zircaloy Cladding in Vacuum and Steam Under Transient Heating Conditions: Summary Report, in NUREG-0344, U.S. NRC.
Darchis, L., Lemoine, P., 1984. EDGAR FROID Gaines Framatome, modélisation de la déformation des gaines en zircaloy dans des conditions d'un accident de perte de réfrigérant primaire, critère de rupture. Note technique SRMA 84-1346.
Dif, B., et al., 2023. Reassessment of FRAPTRAN's cladding failure criteria in Loca within R2CA H2020 project. Springer Proc. Phys. 299, 97–107.
Dominguez, C., et al. (2022). Fuel Cladding Deformation During LOCA: Comparison Between Single-rod and Multi-rod tests. NENE conference September 2022. Portoroz, Slovenia.
Erbacher, F.J., et al., 1997. Temperaturtransiente Kriechberstversuche an Zirconium-Niob1-Hüllrohren – Vergleich zu Zircaloy-4 Hüllrohren. FZKA 5726.
Forgeron, T., et al., 2000. Experiment and Modeling of Advanced fuel rod Cladding Behavior Under LOCA Conditions: Alpha-beta Phase Transformation Kinetics and EDGAR Methodology. ASTM Special Technical Publication(1354) 256–278.
Glantz, T., et al., 2017. DRACCAR: a multi-physics code for computational analysis of multi-rod ballooning and fuel relocation during LOCA transients Part two: Assessment of modeling capabilities. NED.
Glantz, T., et al., DRACCAR: a multi-physics code for computational analysis of multi-rod ballooning and fuel relocation during LOCA transients. Part one : General modeling description. Nuclear Engineering and Design, 2017.

Jacq, F., Taurines, T., 2021. Zy-4 LOCA cladding burst criteria computed by a neural network. Nucl. Eng. Des. 385.
Kaddour, D., et al., 2004. Experimental determination of creep properties of zirconium alloys together with phase transformation. Scripta Comput. Sci. Appl. Math. Materialia 51 (6), 515–519.
Karb, E.H., et al., LWR Fuel Rod Behavior in the FR2 ln-pile Tests Simulating the Heatup Phase of a LOCA. Final Report. KFK 3346, 1983.
Nuclear Fuel Behaviour in Loss-of-Coolant Accident (LOCA) Conditions, 2009, NEA No. 6846, NEA.
Markiewicz, M.E. and F.J. Erbacher, Experiments on ballooning in pressurized and transiently heated Zircaloy-4 tubes, KfK Technical Report 4343, 1988.
Massih, A.R., 2009. Transformation kinetics of zirconium alloys under non-isothermal conditions. J. Nucl. Mater. 384 (3), 330–335.
Massih, A.R., Jernkvist, L.O., 2015. Assessment of Data and Criteria for Cladding Burst in Loss-of-Coolant Accidents 46, 2015.
Meyer, R.O., Wiesenack, W., 2022. A critique of fuel behavior in LOCA safety analyses and a proposed alternative. Nucl. Eng. Design 394.
Mohr, C.L., et al., LOCA Simulation in the National Research Universal Reactor Program. Data Report for the Third Materials Experiment (MT-3), NUREG/CR-2528, 1983.
Nagase, F., Fuketa, T., 2006. Fracture Behavior of Irradiated Zircaloy-4 Cladding under Simulated LOCA Conditions. J. Nucl. Sci. Technol. 43 (9), 1114–1119.
Nagy, R., et al., 2018. Optical observation of the ballooning and burst of E110 and E110G cladding tubes. Nucl. Eng. Design 339.
Perez-Feró E. et al.: Experimental Database of E110 Claddings under Accident Conditions, EK-FRL-2012-255-01/02 (2013).
Powers, D.A., Meyer, R.O., 1980. Cladding Swelling and Rupture Models for LOCA Analysis, in NUREG-0630, U.S. NRC.
Repetto, G., et al., The R&D PERFROI project on thermal mechanical and thermal hydraulics behaviors of a fuel rod assembly during a Loss Of Coolant Accident, in NURETH, International Topical Meeting on Nuclear Reactor Thermal Hydraulics2016: Chicago.
Report on Fuel Fragmentation, Relocation and Dispersal, NEA/CSNI/R(2016)16, 2016.
Rosinger, H.E., 1984. A model to predict the failure of zircaloy-4 fuel sheathing during postulated loca conditions. J. Nucl. Mater. 120 (1), 41–54.
Sawarn, T.K., et al., 2017. Study of clad ballooning and rupture behaviour of Indian PHWR fuel pins under transient heating condition in steam environment. J. Nucl. Mater. 495, 332–342.
Stuckert, J., et al. First results of the bundle test QUENCH-L2 with M5® claddings. in 19th International QUENCH Workshop. 2013. Karlsruhe.
Stuckert, J., et al. First results of the bundle test QUENCH-L4 with hydrogenated M5® claddings. in 20th International QUENCH Workshop. 2014. Karlsruhe.
Stuckert, J., et al., QUENCH-LOCA-Reports Nr. 1 : Results of the commissioning bundle test QUENCH-L0 performed under LOCA conditions (SR-7571), KIT 2015.
Stuckert, J., et al., Results of the LOCA bundle test QUENCH-L5 with pre-hydrogenated optimised ZIRLO™ claddings (SR-7738), 2018.
Stuckert, J., et al., Results of the reference bundle test QUENCH-L1 with Zircaloy-4 claddings performed under LOCA conditons (SR-7651), 2018.
Stuckert, J., et al., Results of the LOCA bundle test QUENCH-L3 with optimised ZIRLO™ claddings (SR-7737), 2018.
Suman, S., 2021. Influence of hydrogen concentration on burst parameters of Zircaloy-4 cladding tube under simulated loss-of-coolant accident. Nucl. Eng. Technol. 53, 474–483.
Thieurmel, R., Identification des conditions de rupture fragile des gainages combustibles en alliage de zirconium oxydés sous vapeur d'eau à haute température et trempés sous charge axiale., in Paris Sciences et Lettres, 2018.
Wiehr, K. and U. Harten Datenbericht REBEKA-6, KfK 3986, 1986.
Wilson, C.L., et al., Large-Break LOCA, In-Reactor Fuel Bundle Materials Test MT-6A, PNNL-8829, 1993.
Wilson, C.L., et al., LOCA Simulation in NRU Program, Data Report for the Fourth Materials Experiment (MT-4), 1983.
Yadav, A.K., et al., 2018. Experimental and numerical investigation on thermo-mechanical behavior of fuel rod under simulated LOCA conditions. Nucl. Eng. Design 337, 51–65.
Yegorova L. et al.: Data Base on the Behavior of High Burnup Fuel Rods with Zr-1%Nb Cladding and U02 Fuel (VVER Type) under Reactivity Accident Conditions, NUREG/IA-0156 (1999).
Yegorova L. et al.: Mechanical Properties of Unirradiated and Irradiated Zr-1% Nb Cladding, NUREG/IA-0199 (2001).